A double Rydberg anion with a hydrogen bond and a solvated double Rydberg anion: Interpretation of the photoelectron spectrum of $N_2H_7^-$

J. V. Ortiz[a]

Department of Chemistry, Kansas State University, Manhattan, Kansas 66506-3701

A double Rydberg anion has two electrons in diffuse orbitals that are bound by a closed-shell, cationic core. Low-energy features in the recently reported photoelectron spectrum of $N_2H_7^-$ are assigned to double Rydberg anions on the basis of electron propagator calculations employing Brueckner doubles, coupled-cluster reference states. The lowest electron detachment energy, 0.415 eV, corresponds to an initial state consisting of a hydrogen-bridged $N_2H_7^+$ core and two diffuse electrons. A feature at slightly higher energy, 0.578 eV, belongs to a complex that comprises a tetrahedral NH_4^- double Rydberg anion and an ammonia solvent molecule. The most intense peak in the photoelectron spectrum, which occurs at 1.460 eV, pertains to a complex with a hydride anion and two ammonia solvent molecules. Plots of Dyson orbitals associated with electron detachment energies facilitate qualitative interpretation of electronic structure in the anions and in the neutral final states. Vibrational structure associated with each of these features has been interpreted as well. Previous assignments of electron detachment energies to the hydride–ammonia and tetrahedral isomers of NH_4^- have been confirmed with the present methods. Vibrationally excited final states have been assigned for this spectrum also. © *2002 American Institute of Physics.*
[DOI: 10.1063/1.1499492]

I. INTRODUCTION

Double Rydberg anions consist of a closed-shell cationic core and two electrons in diffuse orbitals. Tetrahedral NH_4^- is an example of such an anion, for it consists of an ammonium core and two electrons that occupy a diffuse, a_1 orbital. This orbital's probability density accumulates chiefly outside the peripheral nuclei, for the largest atomic contributions are made by diffuse s functions centered on the hydrogens. A radial node is produced by destructive interference between diffuse s functions on nitrogen and hydrogen. In the united atom limit, NH_4^- forms Na^-, with the diffuse a_1 orbital correlating to the $3s$ atomic level.

Computationally based proposals for a tetrahedral isomer of NH_4^- were published in 1986.[1,2] Soon afterward, Bowen and co-workers proposed that a low-energy peak in the photoelectron spectrum of NH_4^-[3] be assigned to electron detachment from a tetrahedral anion.[4–6] More intense, high-energy features in this spectrum were assigned to a hydride–ammonia complex;[7] a similar description of NH_4^- had accompanied a Fourier-transform, ion–cyclotron spectrum.[8] Electron propagator calculations on the electron detachment energies of the anion–molecule and tetrahedral isomers of NH_4^- confirmed Bowen's interpretation.[9] The sharpness of the low-energy peak was explained by an analysis of the Dyson orbital (see below for the definition of a Dyson orbital) connecting the tetrahedral NH_4^- anion and the corresponding neutral. These conclusions on the diffuseness and nodal structure of the Dyson orbital validated use of the term

"double Rydberg anion."[10] A configuration interaction study provided additional confirmation.[11,12] Matsunaga and Gordon also have confirmed these conclusions and have performed classical trajectory calculations on dissociation pathways.[13]

Alternative cationic cores have been considered theoretically. Among the predicted double Rydberg anions are a pyramidal (C_{3v}) form of OH_3^-[12,14] and tetrahedral PH_4^-.[13,15,16] Dyson orbitals for electron detachment from these anions are qualitatively similar to their tetrahedral NH_4^- counterpart. Substituted double Rydberg anions with the formulas NH_3R^- and OH_2R^- (where R=F, OH, NH_2, and CH_3) were examined recently.[17] Double Rydberg isomers of NH_3OH^-, $NH_3NH_2^-$, $NH_3CH_3^-$, and $OH_2CH_3^-$ were found to be stable minima in their potential energy surfaces and to have positive electron detachment energies. Dyson orbitals pertaining to the least bound electrons of the NH_3R^- and OH_2R^- anions are distributed chiefly outside the N–H and O–H bonds of the tetrahedral nitrogen and pyramidal oxygen atoms.

Photoelectron spectra of $N_nH_{3n+1}^-$ species with $n=1–5$ have recently been recorded.[18] Especially noteworthy in this report is the photoelectron spectrum of $N_2H_7^-$. Here, the peak which is simplest to assign belongs to a hydride that is coordinated to two ammonia molecules. Two additional, low-energy peaks are deployed almost symmetrically about the energetic position of the double Rydberg peak of NH_4^-. The shapes and energies of these features lead to a hypothesis of two $N_2H_7^-$ double Rydberg anions. In this view, one peak belongs to a tetrahedral NH_4^- anion that is coordinated to an ammonia molecule, while the other peak pertains to a

[a]Electronic mail: ortiz@ksu.edu

TABLE I. Total energies (a.u.)

Species	QCISD[a]	ZPE[b]	CCSD(T)[c]
Bridge $N_2H_7^-$	$-113.389\,48$	$0.084\,56$	$-113.467\,68$
$NH_4^-(NH_3)$	$-113.383\,79$	$0.081\,34$	$-113.461\,76$
$H^-(NH_3)_2$	$-113.403\,75$	$0.074\,67$	$-113.488\,54$
Bridge N_2H_7	$-113.377\,68$	$0.084\,08$	$-113.453\,37$
$NH_4(NH_3)$	$-113.364\,98$	$0.080\,48$	$-113.440\,97$
NH_4^-	$-56.949\,75$	$0.045\,98$	$-56.988\,43$
$H^-(NH_3)$	$-56.959\,96$	$0.036\,67$	$-57.004\,82$
NH_4	$-56.934\,90$	$0.045\,22$	$-56.971\,93$
$H(NH_3)$	$-56.929\,70$	$0.034\,94$	$-56.968\,62$
NH_3	$-56.429\,82$	$0.034\,73$	$-56.468\,71$
H^-	$-0.521\,94$		$-0.521\,94$

[a]Optimized QCISD total energy with $6\text{-}311++G(d,p)$ basis augmented with diffuse nitrogen sp and hydrogen s functions.
[b]Zero–point energy at optimized QCISD geometry.
[c]Single–point total energy with $6\text{-}311++G(2df,2p)$ basis augmented with an extra set of diffuse nitrogen sp and hydrogen s functions.

hydrogen-bonded H_3N–H^+–NH_3 core with two diffuse electrons.

To assist in the assignment of this photoelectron spectrum, electron propagator calculations on vertical detachment energies and corresponding Dyson orbitals pertaining to three kinds of $N_2H_7^-$ structures have been performed. Since the recent experimental report also contains more detailed results on the photoelectron spectrum of NH_4^-, the improved electron propagator methods of the present study have been applied to this smaller anion as well.

II. TOTAL ENERGY CALCULATIONS

After preliminary searches with lower levels of theory, structures were optimized with quadratic configuration interaction with single and double excitation (QCISD) total energies[19] and the $6\text{-}311++G(d,p)$ basis[20] augmented with nitrogen diffuse sp (exponent=0.0192) and hydrogen diffuse s functions (exponent=0.0108). Corresponding harmonic frequencies and zero-point vibrational energies were evaluated at all stationary points. These results are summarized in the first three columns of Table I. Single-point energies of neutral species were calculated at the optimized geometries of anions. Table II displays these data.

Coupled-cluster single and double excitation total energies with a perturbative triples correction, CCSD(T),[21,22] were determined at the optimized geometries obtained at the QCISD level. In these calculations, the $6\text{-}311++G(2df,2p)$ basis[20] was augmented by the same diffuse

TABLE II. Neutral total energies at anion-optimized geometries (a.u.).

Molecule	QCISD[a]
Bridge N_2H_7	$-113.377\,46$
$NH_4(NH_3)$	$-113.364\,78$
$H(NH_3)_2$	$-113.357\,50$
NH_4	$-56.934\,89$
$H(NH_3)$	$-56.927\,50$

[a]QCISD total energies at optimized QCISD geometries of anions.

TABLE III. Vertical detachment energies (eV).

Anion	VDE[a]	p[b]
Bridge $N_2H_7^-$	0.415	0.84
$NH_4^-(NH_3)$	0.604	0.90
$H^-(NH_3)_2$	1.489	0.81
NH_4^-	0.481	0.86
$H^-(NH_3)$	1.074	0.80

[a]BD-T1 electron propagator calculation with the $6\text{-}311++G(2df,2p)$ basis augmented with two extra sets of diffuse nitrogen sp and hydrogen s functions.
[b]Pole strength; see Eq. (2).

functions used in the QCISD geometry optimizations. The last column of Table I contains these energies.

GAUSSIAN 98[23] was employed in these calculations. Diagrams of optimized geometries were generated with the MOLDEN program.[24]

III. ELECTRON PROPAGATOR CALCULATIONS

Electron propagator calculations in the BD-T1 approximation[25,26] produced vertical detachment energies of the anions and corresponding pole strengths. Here, the $6\text{-}311++G(2df,2p)$ basis was augmented by two sets of nitrogen diffuse sp (exponents=0.0192, 0.005 76) and hydrogen diffuse s functions (exponents=0.0108, 0.003 24). Results are shown in Table III.

For each vertical electron detachment energy calculated with electron propagator theory,[26–28] there corresponds a Dyson orbital defined by

$$\phi_r^{\text{Dyson}}(x_1) = N^{1/2} \int \Psi_{\text{anion}}(x_1, x_2, x_3, \ldots, x_N)$$
$$\times \Psi_{r,\text{neutral}}^*(x_2, x_3, x_4, \ldots, x_N)$$
$$\times dx_2\, dx_3\, dx_4, \ldots dx_N, \qquad (1)$$

where x_k is the combined space–spin coordinate of electron k, Ψ_{anion} is the anionic, initial state with N electrons, and $\Psi_{r,\text{neutral}}^*$ is the rth, neutral, final state with $N-1$ electrons. Plots of Dyson orbitals disclose how electronic structure changes as a result of electron detachment.
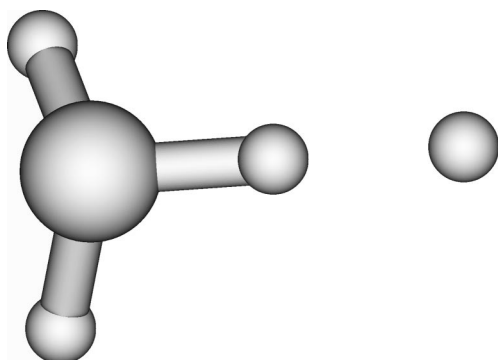
The normalization integral of a Dyson orbital is known as its pole strength, p, where

$$p_r = \int |\phi_r^{\text{Dyson}}(x)|^2 dx. \qquad (2)$$

Pole strengths in general lie between 0 and 1. An alternative expression for the pole strength is

$$p_r = \sum_i^{\text{occ}} |c_{i,r}|^2 + \sum_a^{\text{vir}} |c_{a,r}|^2 \qquad (3)$$

where the c coefficients are taken from the ionization operator

5750   J. Chem. Phys., Vol. 117, No. 12, 22 September 2002

J. V. Ortiz

FIG. 1. Optimized $H^-(NH_3)$ structure.

$$O_r = \sum_i^{occ} c_{i,r} a_i + \sum_a^{vir} c_{a,r} a_a + \sum_{i<j}^{occ} \sum_a^{vir} c_{aij,r} a_a^\dagger a_i a_j$$

$$+ \sum_{a<b}^{vir} \sum_i^{occ} c_{iab,r} a_i^\dagger a_a a_b + \cdots . \qquad (4)$$

In this expression, a_s and $a_s^\dagger$ are annihilation and creation operators, respectively, for the spin–orbital s. The indices $i, j, k, \ldots$ and $a, b, c, \ldots$ correspond to occupied and virtual spin–orbitals, respectively. When pole strengths are close to unity, coefficients corresponding to shake up operators in the third and subsequent terms in the expression for O_r are small and the qualitative validity of a simple, orbital picture for electron detachment to the rth final state is established.

In BD-T1 calculations,[25,26] the electron propagator is expressed in a basis of orbitals from a Brueckner doubles, coupled-cluster wave function.[29,30] This ansatz has a reference determinantal wave function that defines occupied and virtual orbitals.

Electron propagator calculations were performed with a program link that is connected to GAUSSIAN 98.[23] Dyson orbital plots were generated with MOLDEN.[24]

IV. RESULTS AND DISCUSSION

A. Photoelectron spectrum of NH_4^-

1. $H^-(NH_3)$

The dominating feature in the photoelectron spectrum of NH_4^- is a sharp peak at 1.110 eV which is due to detachment of an electron from the hydride of the $H^-(NH_3)$ complex.[3,7,18] In the optimized structure, one of the N–H bonds of the ammonia molecule is directed toward the hydride. (See Fig. 1.) The hydride and bridging hydrogen nuclei are separated by 1.89 Å. Distortions of the coordinated ammonia molecule comprise increased N–H bond lengths and smaller H–N–H bond angles. (See Table IV.) BD–T1 electron propagator calculations predict a vertical detachment energy of 1.074 eV.

Optimization of the neutral, final state's geometry leads to a structure with an increased separation (3.27 Å) between the hydrogen atom and the nearest ammonia hydrogen. The optimized total energy is within 0.2 millihartree of the H $+NH_3$ dissociation limit. Table IV shows that the structure of the NH_3 fragment is identical to that of an uncoordinated

TABLE IV. $H(NH_3)$ and $H^-(NH_3)$ geometries, optimized with QCISD and $6\text{-}311++G(d,p)$ basis augmented with one set of diffuse nitrogen sp and hydrogen s functions.

Parameter	Neutral	Anion	NH_3
$H^- - H_b$	3.266	1.888	
$H^- - H_b - N$	171.6	169.4	
$N - H_b$	1.015	1.036	1.015
$N - H$	1.015	1.020	
$H_b - N - H$	106.9	103.6	106.9
$H - N - H$	106.9	105.5	

ammonia molecule. Vibrational frequencies for NH_3 and for the $H(NH_3)$ modes listed in Table V are practically identical. These data indicate that electron detachment from the $H^-(NH_3)$ complex leads to dissociation into a hydrogen atom and an ammonia molecule.

From the data of Tables I and II, it is possible to infer the relaxation energy along the potential energy surface of the neutral species. In addition, one may consider zero-point energies from Table I. With these corrections, the adiabatic electron detachment energy becomes 0.967 eV. From the CCSD(T) and zero-point energy data of Table I, an alternative value of 0.938 eV may be inferred.

A smaller feature occurs at an energy that is 0.436 eV higher than that of the principal peak.[18] This less intense peak may be assigned to the NH_3 symmetric stretch frequency calculated for the $H(NH_3)$ complex at 3509 cm^{-1}, or 0.435 eV (see Table V). The chief structural difference between free and hydride-coordinated ammonia molecules pertains to the N–H bond that points to the hydride in the anionic complex. Electron detachment thus accesses a vibrationally excited state of ammonia in addition to its ground vibrational state.

The Dyson orbital for vertical electron detachment is dominated by diffuse s functions on the hydride. In Fig. 2, the ± 0.025 contours of this orbital are displayed. Only a small amount of delocalization onto the coordinating ammonia molecule takes place. A pole strength equal to 0.80 indicates that triple field operator products [see Eq. (4)] are relatively important in O_r. The most important operators of this type have the form $a_b^\dagger a_{H-,\alpha} a_{H-,\beta}$, where b is a virtual orbital and the $H-$ subscript stands for an occupied orbital in the Brueckner doubles reference determinant that has an overlap with the Dyson orbital of 0.999. When this kind of triple-field operator acts on the Brueckner reference determinant, both electrons in the diffuse orbital are annihilated and an electron is created in a tighter virtual orbital. Such operators allow the hydride–centered, diffuse s functions to contract in the final, neutral state.

TABLE V. $H(NH_3)$ and $H^-(NH_3)$ harmonic frequencies (cm^{-1}).

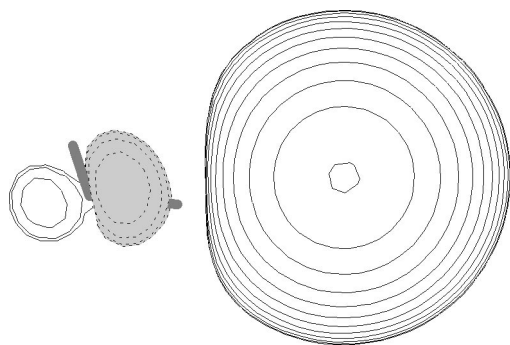| Mode	Neutral	Anion	NH_3
NH_3 umbrella	1096	1263	1097
NH_3 bend	1679,1680	1655,1718	1678
NH_3 sym. stretch	3509	3301	3509
NH_3 asym. stretch	3641,3641	3514,3582	3641

FIG. 2. Dyson orbital for $H^-(NH_3)$ electron detachment, contours $= \pm 0.025$.

2. Tetrahedral NH_4^-

In the low-energy regime, features of considerably less intensity have been discovered.[3–6] A sharp peak at 0.472 eV has been assigned to electron detachment from a tetrahedral NH_4^- species.[18] In BD-T1 calculations, the vertical detachment energy is predicted to be 0.481 eV.

Bond lengths and vibrational frequencies of the tetrahedral anion and neutral radical are listed in Table VI. The energy difference along the NH_4 potential energy surface between the anion and neutral geometries is very small. Differences in zero-point energies between the anion and neutral are somewhat larger. After applying these corrections to the BD-T1 prediction, the 0–0 transition energy becomes 0.460 eV, in excellent agreement with the experimental peak.

A smaller peak in the low-energy regime has been found at 0.651 eV, a shift of 0.179 eV with respect to the previous feature. It may be assigned to the degenerate umbrella modes of NH_4, which occur at 1354 cm^{-1}, or 0.168 eV, in QCISD harmonic frequency calculations.

The Dyson orbital for electron detachment depicted in Fig. 3 is dominated by diffuse functions. The tighter ± 0.03 contours of Fig. 3(a) reveal the nodal structure that is concealed by the ± 0.025 contours of Fig. 3(b). An antibonding relationship between diffuse s functions on nitrogen and the hydrogens creates a node close to the hydrogen nuclei. Most of the corresponding electron density is found outside of the hydrogens. The diffuse character and nodal structure of this Dyson orbital confirm the double Rydberg appellation of the tetrahedral NH_4^- anion. A higher pole strength, 0.86, pertains to this electron detachment. The chief triple-field operator products in O_r have the form $a_b^\dagger a_{Ryd,\alpha} a_{Ryd,\beta}$, where b is a virtual orbital and Ryd is the index of an occupied orbital in the Brueckner doubles reference determinant that has an
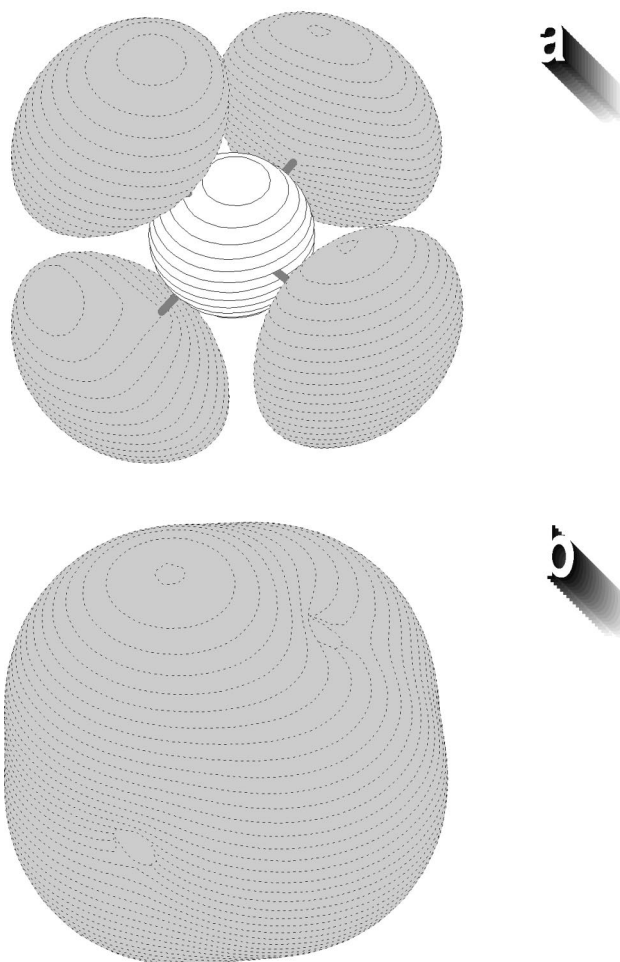
TABLE VI. Tetrahedral NH_4 and NH_4^- geometries and harmonic frequencies (cm^{-1}), optimized with QCISD and 6-311++G(d,p) basis augmented with one set of diffuse nitrogen sp and hydrogen s functions.

	Neutral	Anion
N–H	1.040	1.038
t_2 umbrella	1354	1380
e bend	1616	1615
a_1 sym. stretch	3109	3115
t_2 asym. stretch	3149	3231

FIG. 3. (a) Dyson orbital for tetrahedral NH_4^- electron detachment, contours $= \pm 0.03$. (b) Dyson orbital for tetrahedral NH_4^- electron detachment, contours $= \pm 0.025$.

overlap with the Dyson orbital of 0.999. Relaxation of the double Rydberg orbital is described by this class of operators, as two electrons assigned to this orbital are annihilated, while an electron is created in a high-energy, virtual orbital that is less diffuse.

B. Photoelectron spectrum of $N_2H_7^-$

1. $H^-(NH_3)_2$

In the photoelectron spectrum of $N_2H_7^-$, the principal peak occurs at 1.460 eV.[18] This value is close to the BD-T1 result of 1.489 eV (see Table III) for the vertical detachment energy of the $H^-(NH_3)_2$ complex shown in Fig. 4(a). Each ammonia in this C_2 complex has an N–H bond that points toward the hydride. Two other N–H bonds are aligned with the lone pairs of the opposite ammonia molecules. Table VII lists bond lengths, angles and dihedral angles pertaining to the hydride (H$^-$), bridging ammonia hydrogen (H$_b$), and nonbridging ammonia hydrogen (H) atoms. Refinement of a previously published structure[31] produced a transition state. Geometry optimization of the neutral species that begins with the anion structure leads to a complex of two ammonia molecules plus a well-separated hydrogen atom.
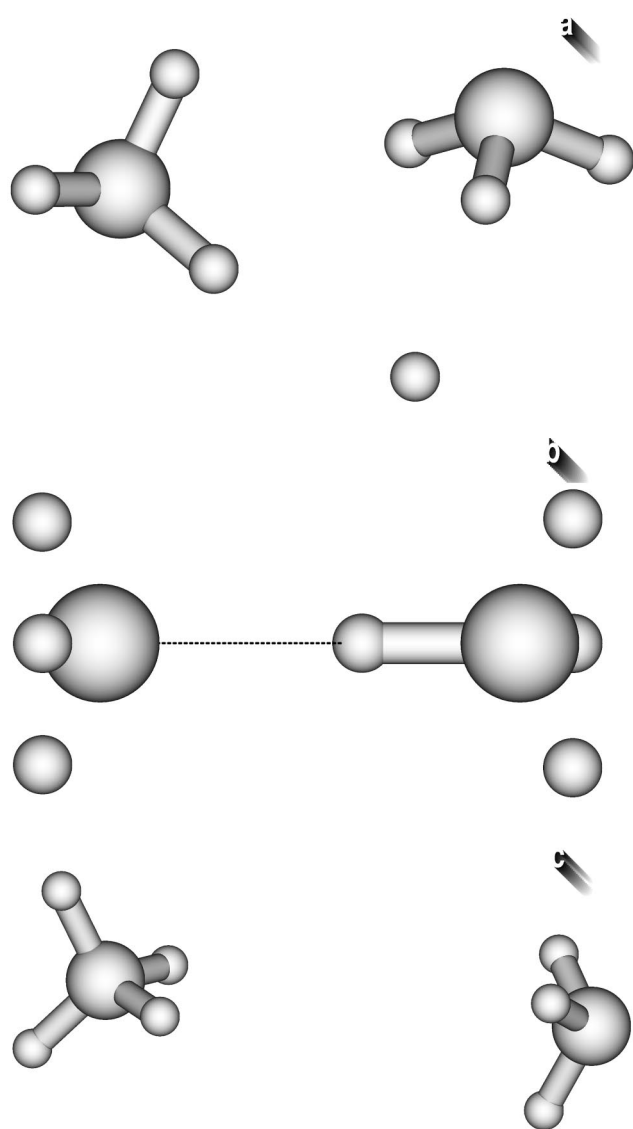
FIG. 4. (a) Optimized $H^-(NH_3)_2$ structure. (b) Optimized bridged $N_2H_7^-$ structure. (c) Optimized $NH_4^-(NH_3)$ structure.

A high-energy feature on the broad, principal peak at 1.896 eV has been discerned.[18] The spacing is 0.436 eV with respect to the principal maximum, just as it was for the analogous peak in the $H^-(NH_3)$ spectrum. (See Table VIII.) This feature therefore is assigned to a vibrationally excited

TABLE VII. $H^-(NH_3)_2$ geometry, optimized with QCISD and 6-311+ +G(d,p) basis augmented with one set of diffuse nitrogen sp and hydrogen s functions.

Parameter	Anion	NH_3
$H^- - H_b$	1.959	
$H_b - H^- - H_b$	72.2	
$H^- - H_b - N$	167.8	
$H^- - H_b - N - H$	9.6, −100.6	
$N - H_b$	1.032	1.015
$N - H$	1.019, 1.019	
$H_b - N - H$	104.1, 104.7	106.9
$H - N - H$	105.1	

TABLE VIII. $H^-(NH_3)_2$ harmonic frequencies (cm^{-1}).

Mode	Anion	NH_3
NH_3 umbrella	1253, 1256	1097
NH_3 bend	1658, 1668, 1709, 1749	1678
NH_3 sym. stretch	3295, 3308	3509
NH_3 asym. stretch	3519, 3520, 3587, 3588	3641

final state corresponding to the NH_3 symmetric stretch mode at 3509 cm^{-1}, or 0.435 eV. For isolated NH_3, the experimental frequency is 3336 cm^{-1}. The discrepancy between these two values is only 0.021 eV.

The Dyson orbital associated with the BD-T1 prediction is shown in Fig. 5. S functions on the hydride nucleus dominate, although a little delocalization onto the solvent molecules may be seen in these ± 0.025 contours. The pole strength of 0.81 is relatively small and indicates a high degree of correlation involving two hydride electrons. Strong orbital relaxation, described by triple-field operators of the form $a_b^\dagger a_{H-,\alpha} a_{H-,\beta}$, is chiefly responsible for the small pole strength. These operators, which have the same form as those discussed above for the electron detachment operator of $H^-(NH_3)$, allow the remaining hydrogenic electron to contract in the final state.

2. H-bridged $N_2H_7^-$

Dilation of the intensity axis in the $N_2H_7^-$ photoelectron spectrum by a factor of 500 reveals several features at low electron binding energy.[18] The lowest of these occurs at 0.415 eV, which also happens to be the BD-T1 value for the vertical detachment energy of the bridged anion of Fig. 4(b). A tetrahedral fragment with a nitrogen and four hydrogen nuclei is linked by a hydrogen bond to an ammonia fragment in a C_{3v} structure that resembles $N_2H_7^+$. Table IX displays the two internuclear separations that pertain to the bridging
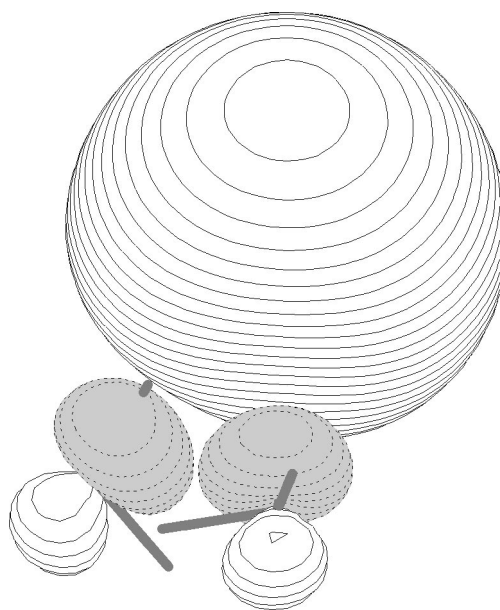

FIG. 5. Dyson orbital for $H^-(NH_3)_2$ electron detachment, contours $= \pm 0.025$.

TABLE IX. N_2H_7 and $N_2H_7^-$ bridge geometries, optimized with QCISD and 6-311++G(d,p) basis augmented with one set of diffuse nitrogen sp and hydrogen s functions.

Parameter[a]	Neutral	Anion	NH_3	NH_4	NH_4^-
N–H_b (H bond)	1.847	1.761			
N–H_b (NH_4)	1.054	1.064			
N–H (NH_4)	1.036	1.032		1.040	1.038
N–H (NH_3)	1.019	1.021	1.015		
H_b–N–H (NH_4)	110.2	110.1			
H_b–N–H (NH_3)	112.4	112.4			
H–N–H (NH_4)	108.7	108.8		109.5	109.5
H–N–H (NH_3)	106.4	106.5	106.9		

[a]H_b designates the bridging hydrogen of Fig. 4(b); nonbridging hydrogens are associated with the tetrahedral fragment (NH_4) or with the ammonia fragment (NH_3).

hydrogen, which designated H_b. Vibrational frequencies, shown in Table X, do not differ markedly from those of the isolated fragments, except for the mode at 2734 cm^{-1} which pertains to the stretching of the N–H_b bond.

Optimization of the final, neutral state produces a longer hydrogen bond and a shorter N–H_b bond length. Other geometrical parameters, in contrast, change very little with respect to the anion values. The stretching mode for the N–H_b bond acquires a higher frequency in the neutral state.
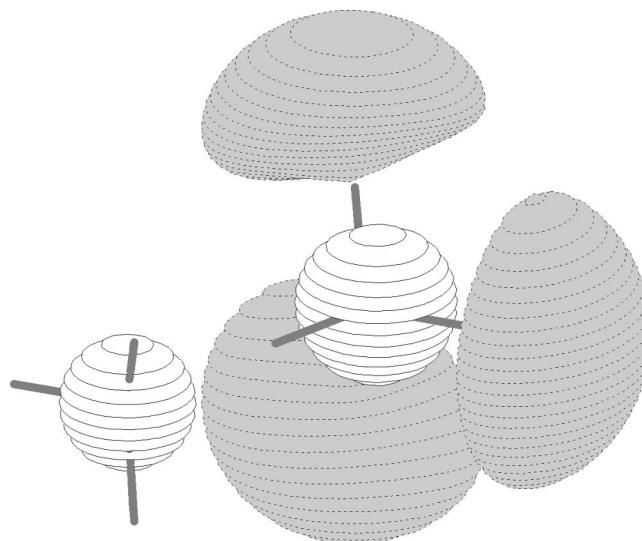
After applying relaxation and zero-point corrections that follow from the data of Tables I and II, the 0–0 transition energy is predicted to be 0.396 eV. Using the CCSD(T) total energies for the adiabatic transition energy and applying the same zero-point corrections yields a 0–0 transition energy of 0.386 eV.

A less intense feature at 0.723 eV is shifted by 0.308 eV with respect to the lowest transition energy.[18] Since the main discrepancies between the anion and neutral bridge structures occur in the hydrogen bond length and the N–H_b distance, the calculated N_2H_7 mode at 2938 cm^{-1} (0.364 eV) corresponding chiefly to the stretching of the bridging N–H_b bond is assigned to this feature. Corrections to the harmonic approximation are likely to be significant here, for the barrier between the anionic bridge geometry and a symmetric, D_{3d} transition state is only 0.141 eV in QCISD calculations. The present overestimate of the shift, 0.056 eV, therefore may be attributed to neglect of anharmonic corrections.

TABLE X. N_2H_7 and $N_2H_7^-$ bridge harmonic frequencies (cm^{-1}).

Mode[a]	Neutral	Anion	NH_3	NH_4	NH_4^-
a_1 NH_3 umbrella	1207	1198	1097		
a_1 NH_4 H_n umbrella	1353	1374		1354	1380
e NH_4 umbrella	1440	1482			
e NH_3 bend	1643	1622	1678		
e NH_4 bend	1677	1689		1616	1615
a_1 H_b stretch	2938	2734			
a_1 NH_4 H_n stretch	3188	3258		3109	3115
e NH_4 H_n stretch	3255	3349		3149	3231
a_1 NH_3 stretch	3466	3423	3509		
e NH_3 stretch	3595	3559	3641		

[a]H_b designates the bridging hydrogen of Fig. 4(b); H_n designates nonbridging hydrogens associated with the tetrahedral fragment (NH_4).

FIG. 6. Dyson orbital for bridged $N_2H_7^-$ electron detachment, contours $= \pm 0.025$.

Another small peak at 0.894 eV also may be explained by vibrational excitation in the final state. Symmetric and asymmetric NH_3 stretching modes in the bridge N_2H_7 structure have been calculated at 3466 and 3595 cm^{-1}, respectively. Since these values are equivalent to 0.430 and 0.446 eV, they are in close agreement with the experimentally reported spacing, 0.479 eV, between this peak and the lowest transition energy. The latter figure may be an overestimate, for the overwhelming intensity of the principal feature at 1.460 eV may lead to a bias in the location of a minor peak maximum.

The Dyson orbital corresponding to the vertical detachment energy is concentrated at the periphery of the three, nonbridging N–H_n bonds of the tetrahedral fragment. Diffuse functions on these hydrogens make the largest contributions. Contour values of ± 0.025 are shown in Fig. 6. A node occurs between the N and H_n nuclei of the tetrahedron. Some delocalization onto the ammonia nitrogen is present as well. Similar distributions of amplitudes have been seen in the substituted double Rydberg anions, $NH_3CH_3^-$, $NH_3NH_2^-$, and NH_3OH^-.[17] The pole strength is 0.84 and the shake up operators with the largest coefficients in O_r have the form $a_b^\dagger a_{\mathrm{Ryd},\alpha} a_{\mathrm{Ryd},\beta}$, where b is a virtual orbital and Ryd designates an occupied Brueckner orbital with an overlap of 0.999 with the Dyson orbital. Orbital relaxation, in which the diffuse orbital contracts in the neutral final state, is chiefly responsible for the reduction of the pole strength from unity.

Triplet bridged structures with D_{3d} and C_{3v} point groups were considered. Optimization of the former produces a high-lying transition state and the latter yields a minimum that is 0.26 eV higher than the singlet.

3. NH_4^-(NH_3)

At 0.578 eV, there is another peak with intensity comparable to the one at 0.415 eV.[18] The vertical detachment energy of the NH_4^-(NH_3) structure of Fig. 4(c) is 0.604 according to BD-T1 electron propagator calculations. This C_s structure has two bridging hydrogen nuclei on the NH_4^- frag-

TABLE XI. $NH_4(NH_3)$ and $NH_4^-(NH_3)$ geometries, optimized with QCISD and $6-311++G(d,p)$ basis augmented with one set of diffuse nitrogen sp and hydrogen s functions.

Parameter[a]	Neutral	Anion	NH_3	NH_4	NH_4^-
N–H$_b$ (NH_4)	1.041	1.040		1.040	1.038
N–H$_n$ (NH_4)	1.040	1.039			
N–H (NH_3)	1.015	1.017	1.015		
H$_b$–N–H$_b$	109.3	109.4		109.5	109.5
H$_n$–N–H$_n$	109.6	109.6			
H$_b$–N–H$_n$	109.4	109.4			
H–N–H (NH_3)	106.8	105.1	106.9		
H–H$_b$	4.453	4.102			
N–N	5.295	4.915			
N–N–H$_b$	57.1	54.9			
H–N–N–H$_b$	76.4	86.4			

[a]H$_b$ and H$_n$ refer, respectively, to the bridging and nonbridging hydrogens of the NH_4^- fragment; H refers to hydrogens on the NH_3 fragment.

ment. All three hydrogens in the NH_3 fragment point toward the anion. Between the NH_4^- and NH_3 fragments, the shortest internuclear separation (see Table XI) is 4.102 Å. Each fragment's structure and vibrational frequencies (see Table XII) are almost undisturbed with respect to their uncoordinated counterparts.

Optimization of the neutral final state leads to an increased separation of the fragments. The total energy is nearly identical to that of the NH_3+ tetrahedral NH_4 dissociation limit. Correcting for relaxation and zero-point energies yields an adiabatic detachment energy of 0.575 eV. The CCSD(T) adiabatic transition energy, updated with the zero-point corrections obtained with QCISD, produces a similar value, 0.542 eV.

The last small peak noted in the experimental report[18] lies at 0.757 eV and therefore is shifted by 0.179 eV with respect to the previous feature. This shift is identical to that seen in spectrum of NH_4^-, where peaks at 0.472 and 0.651 eV have been attributed to electron detachments from a tetrahedral anion. Vibrational frequencies for the solvated, tetrahedral radical, $NH_4(NH_3)$ are calculated at 1354, 1355, and 1356 cm^{-1}. For the bare, tetrahedral radical, the triply degenerate umbrella mode's harmonic frequency is predicted to be 1354 cm^{-1}. No significant change in these frequencies is produced by the coordinating ammonia molecule in the experiment or in the calculations. The value 1354 cm^{-1} equals 0.168 eV, in excellent agreement with the observed shift.

The Dyson orbital for the vertical detachment energy of the $NH_4^-(NH_3)$ structure is similar to its counterpart for bare, tetrahedral NH_4^-. Figures 7(a) and 7(b), respectively, show the ±0.03 and ±0.025 contours. Diffuse functions on the hydrogens of the tetrahedron have the largest coefficients. A node occurs just inside the hydrogen nuclei. Delocalization onto the coordinated NH_3 molecule is small. A large pole strength, 0.90, confirms the orbital description of the electron detachment. In the ionization operator, O_r, the largest shakeup operator coefficient belongs to an operator of the $a_b^\dagger a_{\text{Ryd},\alpha} a_{\text{Ryd},\beta}$ type. Final state, orbital relaxation effects are described by this kind of operator.

C. BD-T1 Dyson orbitals and electron detachment energies

In the hydride complexes, $H^-(NH_3)_n$, the Dyson orbital for electron detachment is centered on the hydride nucleus. For each of the remaining anionic structures, two electrons are assigned to a diffuse orbital that is clearly separated from the other occupied orbitals. The nodal structure of these diffuse orbitals in NH_4^- and $NH_4^-(NH_3)$ resembles that of the highest occupied s orbital of Na^-. A similar pattern is obtained in the bridged $N_2H_7^-$ isomer, but the chief diffuse contributions are located only on the three nonbridging hydrogens of the tetrahedral fragment. The latter is the first example of a double Rydberg anion with a hydrogen-bonded core.

The success of the BD-T1 electron propagator approximation in predicting the vertical electron detachment energies of the anions is founded on the exactness of this approximation for two-electron systems and on its size consistency. The Rydberg electron pair and the hydride electron pair are well separated from the other electrons. One may consider double Rydberg anions to be complexes of a molecular, cationic core with two peripherally delocalized electrons. The Brueckner doubles, coupled-cluster wave function used for the reference state is exact for separated pairs of electrons such as might be encountered in a dilute He or H_2 gas. In the BD-T1 approximation, this reference state is combined with an operator manifold with all simple and triple ($2ph$ and $2hp$) field operators.[25,26] (Electron detachments from two-electron systems cannot involve more complex operators, such as those described by $3h2p$ operators.) Processes involving electron detachment from an occupied orbital accompanied by a single excitation therefore

TABLE XII. $NH_4(NH_3)$ and $NH_4^-(NH_3)$ harmonic frequencies (cm^{-1}).

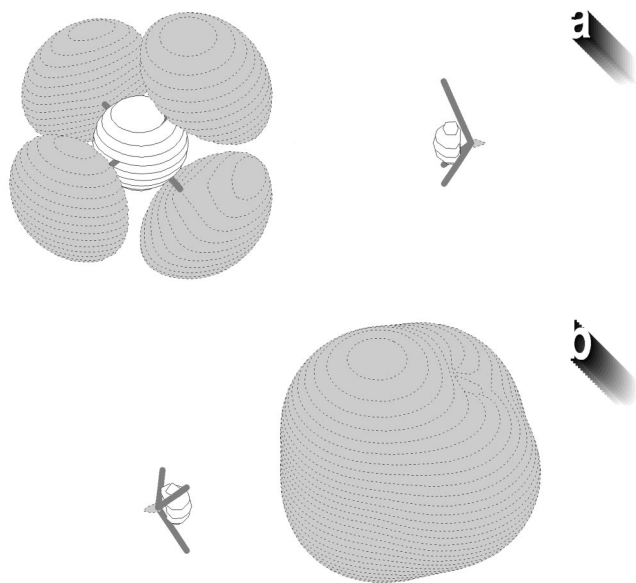| Mode	Neutral	Anion	NH_3	NH_4	NH_4^-
NH_3 umbrella	1098	1178	1097		
NH_4 H$_n$ umbrella	1354,1355,1356	1375,1376,1378		1354	1380
NH_4 bend	1615,1618	1612,1622		1616	1615
NH_3 bend	1680,1680	1680,1680	1678		
NH_4 sym. H$_n$ stretch	3107	3098		3109	3115
NH_4 asym. H$_n$ stretch	3136,3146,3155	3205,3213,3222		3149	3231
NH_3 sym. stretch	3506	3491	3509		
NH_3 asym. stretch	3638,3638	3609,3610	3641		

FIG. 7. (a) Dyson orbital for $NH_4^-(NH_3)$ electron detachment, contours $= \pm 0.03$ (b) Dyson orbital for $NH_4^-(NH_3)$ electron detachment, contours $= \pm 0.025$.

are included and description of final state orbital relaxation is accomplished by this means.

D. Thermochemistry

Relative energies of the anionic minima and dissociation energies may be inferred from the CCSD(T) total energies and QCISD zero-point energies of Table I. $H^-(NH_3)_n$ complexes, where $n=1,2$, are stable with respect to the corresponding $H^- + n\,NH_3$ dissociation limits. (See Table XIII.) The dissociation energy for the $n=2$ complex (0.65 eV) is approximately twice that of the $n=1$ complex (0.33 eV). These values are close to experimentally based upper bounds of 0.71 and 0.36 eV for $n=2$ and $n=1$, respectively.[3] Coordination of an ammonia to tetrahedral NH_4^- lowers the total energy by a smaller amount, 0.11 eV. The more concentrated charge of the hydride anion accounts for this contrast. Approximately 0.70 eV separates the $H^-(NH_3)$ complex from the less stable, tetrahedral anion, NH_4^-. $H^-(NH_3)_2$ is 0.91 eV more stable than the $NH_4^-(NH_3)$ complex and is 0.83 eV more stable than the hydrogen-bridged $N_2H_7^-$ species.

Similar calculations for neutral species imply that there is very little binding energy for complexation of hydrogen atoms to ammonia molecules. Except for the case of the bridged anion, electron detachment leads to dissociation into fragments. The bridged N_2H_7 species is the only neutral structure that lies below (by 0.36 eV) the dissociation limit of $H + 2NH_3$. Tetrahedral NH_4 is approximately 0.2 eV less stable than the $H + NH_3$ dissociation limit.

E. Structural trends

In the bridged $N_2H_7^-$ structure, most of the bond lengths and angles of the tetrahedral, H-donor fragment and of the ammonia fragment closely resemble those of the corresponding, dissociated species. Only the bond lengths pertain-

TABLE XIII. Relative energies of anions.

Anion	a.u.[a]	eV
Bridged $N_2H_7^-$	$-113.383\,12$	0.18
$NH_4^-(NH_3)$	$-113.380\,42$	0.26
$H^-(NH_3)_2$	$-113.413\,87$	-0.65
$NH_4^- + NH_3$	$-113.376\,43$	0.37
$H^-(NH_3) + NH_3$	$-113.402\,13$	-0.33
$H^- + 2NH_3$	$-113.389\,90$	0.00

[a]Sum of CCSD(T) total energies and QCISD zero-point energies.

ing to the bridging hydrogen, H_b, are significantly distorted. Electron detachment reduces the length of the covalent $N\text{--}H_b$ bond by 0.01 Å, but the hydrogen bond is elongated by 0.086 Å.

Two of the four hydrogens of tetrahedral NH_4^- point indirectly toward the hydrogens of the coordinating ammonia molecule in the $NH_4^-(NH_3)$ complex. A long distance, 4.10 Å, separates these hydrogens. Each of the fragments has an internal structure that is almost completely undisturbed by the other's presence.

V. CONCLUSIONS

Electron propagator calculations provide highly accurate assignments of the principal features of the photoelectron spectra of $N_2H_7^-$ and NH_4^-. Vertical detachment energies for $H^-(NH_3)_2$, $NH_4^-(NH_3)$, and hydrogen-bonded $N_2H_7^-$ isomers provide a consistent explanation for the relatively intense, high-energy peak and for the two most intense peaks found in the low-energy regime. Vibrational satellites pertaining to all three cases have been assigned successfully as well. Coordination to an ammonia molecule increases the electron detachment energy of a tetrahedral NH_4^- anion, but formation of a hydrogen bond between the ammonia and tetrahedral fragments leads to a lower value.

Double Rydberg anions possess a novel kind of electron pair. In these species, two electrons are assigned to orbitals that are spread over the periphery of a molecular cation. In this report, the double Rydberg concept is extended beyond simple hydrides, such as tetrahedral NH_4^- or pyramidal OH_3^-, and their substituted analogs, such as NH_3R^- ($R = CH_3$, NH_2, OH) or $OH_2CH_3^-$. A solvated species, $NH_4^-(NH_3)$, consists of a tetrahedral double Rydberg anion that is coordinated to an ammonia molecule through electrostatic interactions. The Dyson orbital for electron detachment is localized on the tetrahedral fragment and strongly resembles its counterpart for tetrahedral NH_4^-. A more stable double Rydberg anion has a hydrogen-bonded $N_2H_7^+$ core. In the Dyson orbital for electron detachment from the bridged $N_2H_7^-$ species, the largest amplitudes are found on the three nonbridging hydrogens of the tetrahedral fragment.

[1] H. Cardy, C. Larrieu, and A. Dargelos, Chem. Phys. Lett. **131**, 507 (1986).

[2] D. Cremer and E. Kraka, J. Phys. Chem. **90**, 33 (1986).

[3] J. T. Snodgrass, J. V. Coe, C. B. Freidhoff, K. M. McHugh, and K. H. Bowen, Faraday Discuss. Chem. Soc. **86**, 241 (1988).

[4] J. T. Snodgrass, Ph.D. dissertation, Johns Hopkins University, 1986.

[5] J. V. Coe, Ph.D. dissertation, Johns Hopkins University, 1986.

[6] S. T. Arnold, J. G. Eaton, D. Patel-Misra, H. W. Sarkas, and K. H. Bowen, in *Ion and Cluster Ion Spectroscopy and Structure*, edited by J. P. Maier (Elsevier, Amsterdam, 1988), p. 147.

[7] J. V. Coe, J. T. Snodgrass, C. B. Freidhoff, K. M. McHugh, and K. H. Bowen, J. Chem. Phys. **83**, 3169 (1985).

[8] J. C. Kleingeld, S. Ingemann, J. E. Jalonen, and N. M. M. Nibbering, J. Am. Chem. Soc. **105**, 2474 (1983).

[9] J. V. Ortiz, J. Chem. Phys. **87**, 3557 (1987).

[10] For a review of double Rydberg anions, see J. Simons and M. Gutowski, Chem. Rev. **91**, 669 (1991).

[11] M. Gutowski, J. Simons, R. Hernández, and H. L. Taylor, J. Phys. Chem. **92**, 6179 (1988).

[12] M. Gutowski and J. Simons, J. Chem. Phys. **93**, 3874 (1990).

[13] N. Matsunaga and M. S. Gordon, J. Phys. Chem. **99**, 12773 (1995).

[14] J. V. Ortiz, J. Chem. Phys. **91**, 7024 (1989).

[15] J. V. Ortiz, J. Phys. Chem. **94**, 4762 (1990).

[16] J. Moc and K. Morokuma, Inorg. Chem. **33**, 551 (1994).

[17] H. Hopper, M. Lococo, O. Dolgounitcheva, V. G. Zakrzewski, and J. V. Ortiz, J. Am. Chem. Soc. **122**, 12813 (2000).

[18] S.-J. Xu, J. M. Niles, J. H. Hendricks, S. A. Lyapustina, and K. H. Bowen, J. Chem. Phys. **117**, 5742 (2002), preceding paper.

[19] J. A. Pople, M. Head-Gordon, and K. Raghavachari, J. Chem. Phys. **87**, 5968 (1987).

[20] R. Krishnan, J. S. Binkley, R. Seeger, and J. A. Pople, J. Chem. Phys. **72**, 650 (1980), and references therein; M. J. Frisch, J. A. Pople, and J. S. Binkley, *ibid.* **80**, 3265 (1984); T. Clark, J. Chandrasekhar, G. W. Spitznagel, and P. v. R. Schleyer, J. Comput. Chem. **4**, 294 (1983).

[21] G. D. Purvis and R. J. Bartlett, J. Chem. Phys. **76**, 1910 (1982).

[22] K. Ragavachari, G. W. Trucks, J. A. Pople, and M. Head-Gordon, Chem. Phys. Lett. **157**, 479 (1989).

[23] M. J. Frisch, G. W. Trucks, H. B. Schlegel, GAUSSIAN 98 (Revision A8) Gaussian, Inc., Pittsburgh, PA, 1998.

[24] G. Schaftenaar, MOLDEN, CAOS/CAMM Center, The Netherlands, 1998.

[25] J. V. Ortiz, Chem. Phys. Lett. **296**, 494 (1998); **297**, 193 (1998).

[26] J. V. Ortiz, Adv. Quantum Chem. **35**, 33 (1999).

[27] J. V. Ortiz, in *Computational Chemistry: Reviews of Current Trends*, edited by J. Leszczynski (World Scientific: Singapore, 1997), Vol. 2, p. 1.

[28] J. V. Ortiz, V. G. Zakrzewski, and O. Dolgounitcheva, in *Conceptual Trends in Quantum Chemistry*, edited by E. S. Kryachko (Kluwer, Dordrecht, 1997), Vol. 3, p. 465.

[29] R. A. Chiles and C. A. Dykstra, J. Chem. Phys. **74**, 4544 (1981).

[30] N. C. Handy, J. A. Pople, M. Head-Gordon, K. Ragavachari, and G. W. Trucks, Chem. Phys. Lett. **164**, 185 (1989).

[31] S. Roszak, J. Chem. Phys. **105**, 7569 (1996).